

# Bayesian Morphology: Fast Unsupervised Bayesian Image Analysis

Florence FORBES and Adrian E. RAFTERY

We consider the problems of image segmentation and classification, and image restoration when the true image is made up of a small number of (unordered) colors. Our emphasis is on both performance and speed; speed has become increasingly important for analyzing large images and multispectral images with many bands, processing large image databases, real-time or near real-time image analysis, and the online analysis of video. Bayesian image analysis provides an elegant solution to these problems, but it is computationally expensive, and the solutions it provides may be sensitive to unrealistic global properties of the models on which it is based. The ICM algorithm is faster and based on the *local* properties of the models underlying Bayesian image analysis; parameter estimation is performed iteratively via pseudolikelihood. Mathematical morphology is faster again and is widely considered to perform well, but lacks a statistical basis: method selection (analogous to parameter estimation) is done in a rather ad hoc manner. We propose *Bayesian morphology*, a synthesis of these methods that attempts to combine the speed of mathematical morphology with the principled statistical basis of ICM. The key observation is that when the original image is discrete (or if an initial segmentation has been carried out), then, assuming a Potts model for the true scene and channel transmission noise, (1) the ICM algorithm is equivalent to a form of mathematical morphology and (2) the segmentation is insensitive to the precise values of the model parameters. Unlike in standard Bayesian images analysis and ICM, it is feasible to do maximum likelihood estimation of the parameters in this setting. For gray-level or multispectral images, we propose an initial segmentation based on the EM algorithm for a mixture model of the marginal distribution of the pixels. The resulting algorithm is much faster than ICM, with gains that increase for more bands and larger images, and has good performance in experiments and for real examples.

**KEY WORDS:** Bayesian image restoration; Iterated conditional mode; Mathematical morphology; Potts model; Pseudolikelihood.

## 1. INTRODUCTION

We consider the problem of image segmentation or classification, or of image restoration when the true scene is made up of a small number of unordered colors. Here we consider only the generic version of this problem, where precise knowledge of the kinds of objects sought is not available; only a general sort of local smoothness similar to that expected by the human eye is assumed.

We consider both performance and speed as criteria for assessing methods. Speed has become increasingly important as the demands on image processing systems have increased over the past 15 years. It is particularly important for analyzing large images; for processing large databases or archives of images; for analyzing multispectral images with many bands, for analyzing real-time, near-real-time, or interactive images; and for analyzing video, either online or off line.

Bayesian image analysis was proposed as a solution to this problem by Geman and Geman (1984), who introduced the Gibbs sampler for finding the posterior mode of the entire true scene, based on a Markov random field probability model. This is a fully statistically grounded method, but it is very computationally expensive. Besag (1986) proposed the iterated conditional modes (ICM) algorithm, which is based on the same model as the methods of Geman and Geman (1984) but uses only the local properties of their model and is faster. The parameters of the model are typically assigned by the user, estimated offline from training data if these are available, or estimated iteratively using maximum pseudolikelihood. Exact maximum likelihood is

typically intractable.

Mathematical morphology was introduced to solve the same general class of problems by Matheron (1975) (see also Serra 1982). It consists of applying sequences of morphological operators such as erosions, dilations, openings, and closings to the image in an order determined by the user. It is very fast and has been much used, and it has been widely reported to perform well in practice. However, it does not have a statistical basis, and so its inferential foundation is uncertain. One consequence of this is that specification of the sequence of operations to be used in any given application tends to be somewhat ad hoc, being based on trial and error on the part of the user.

Although Bayesian image analysis and mathematical morphology are aimed at closely related problems, they have largely developed in isolation from one another. Here we introduce an approach called *Bayesian morphology*, which aims to combine the power, elegance, and firm statistical foundation of Bayesian image analysis with the speed of mathematical morphology, while retaining the good performance of both. Our key observation comes from considering the situation in which the original image to be analyzed consists of the same colors as the true scene, but is a degraded version of it. This can also arise where the original image is gray-scale or multispectral, but an initial, lower-quality segmentation has been performed. Then, if restoration is based on a Potts model for the true scene and the assumption of channel transmission noise, (1) ICM is equivalent to a form of mathematical morphology, and (2) the restoration is the same for a range of values of the model parameters.

Property (1) allows us to perform an ICM restoration using the very fast computational tools of mathematical

Florence Forbes is Research Scientist, Project IS2, INRIA Rhone-Alpes, Monbonnot St. Martin 38330, France (E-mail: [florence.forbes@inrialpes.fr](mailto:florence.forbes@inrialpes.fr)). Adrian E. Raftery is Professor of Statistics and Sociology, Department of Statistics, University of Washington, Seattle, WA 98195 (E-mail: [raftery@stat.washington.edu](mailto:raftery@stat.washington.edu)).

morphology, whereas property (2) allows us to incorporate parameter estimation at a low computational cost. It also allows us to do maximum likelihood estimation of the parameters, which is not feasible in standard Bayesian images analysis and ICM. When the original image is gray-scale or multispectral, we propose initializing the method by positing a finite mixture model for the marginal distribution of (possibly multivariate) pixel intensities, and estimating this using the EM algorithm. We call this *marginal mixture EM segmentation*.

The resulting method is much faster than ICM, and in our experiments with synthetically degraded and real images its performance was comparable to that of ICM. The method can be viewed as a special case of either ICM or mathematical morphology. As a morphological method, it has the advantage in that the sequence of operators is chosen automatically and in a statistically principled manner via the parameter estimation in ICM, rather than in the usual ad hoc manner. The structuring element (morphology) is essentially equivalent to the neighborhood (ICM), which in turn corresponds to the probability model for the true scene. Thus the choice of structuring element can be reduced to a standard problem of statistical model selection, and solved, for example, using Bayesian model selection (Ji and Seymour 1996; Kass and Raftery 1995).

A simple "ancestor" of our approach is to first classify each pixel according to the maximum likelihood classifier, postprocess this using the median filter or simple majority vote local smoother, and iterate until convergence. We call this method "blind restoration." Besag (1986) pointed out that this method has the clear disadvantage of losing track of the records themselves, a criticism that also applies to relaxation labeling methods (Hummel and Zucker 1983; Rosenfeld, Hummel, and Zucker 1976). This is correct, and blind restoration tended to perform relatively poorly in our own experiments, as we report later. However, when simple majority vote is replaced by discrete-image ICM, and naive maximum likelihood is replaced by marginal mixture EM segmentation, this disadvantage seems to no longer have serious practical consequences and often may be more than offset by the increase in speed.

In Section 2 we review the Bayesian, ICM, and morphological approaches. In Section 3 we introduce Bayesian morphology. We describe, online parameter estimation in Section 4, using likelihood and pseudolikelihood criteria. We present various experiments in Section 5, including extensions of Bayesian morphology to gray-scale and multispectral images via marginal mixture EM segmentation. Finally, we discuss connections to other work and possible extensions in Section 6.

## 2. BACKGROUND: BAYESIAN IMAGE ANALYSIS, ITERATED CONDITIONAL MODES, AND MATHEMATICAL MORPHOLOGY

### 2.1 Bayesian Image Restoration and the Iterated Conditional Modes Algorithm

Bayesian image analysis is based on probability models. It includes a variety of tasks, including image restoration.

The true but unknown scene,  $x = \{x_i, i \in S\}$ , where  $S$  is a set of pixels, is interpreted as a particular realization of a random vector  $\mathbf{X}$ . The observed image  $y$  is interpreted as a realization of a random vector  $\mathbf{Y}$  that can be seen as a degraded version of  $\mathbf{X}$ . The vector  $\mathbf{Y}$  depends on  $\mathbf{X}$  through a known conditional probability density function  $\mathcal{L}(y|x)$ , which incorporates the image formation model and the noise model.

To restore  $\mathbf{X}$  is to propose an estimator  $\hat{\mathbf{X}} = \hat{\mathbf{X}}(\mathbf{Y})$  of  $\mathbf{X}$  on the basis of  $\mathbf{Y}$ . Bayesian image restoration methods are based on the following principles. The true image  $x$  is supposed to be a realization of a random field with distribution  $\mathbb{P}(x)$ . Then the restored image  $\hat{x}$  is based on the posterior density of  $x$ , namely  $\mathbb{P}(x|y) \propto \mathcal{L}(y|x)\mathbb{P}(x)$ . A standard restoration criterion consists of maximizing this density, leading to the maximum a posteriori (MAP) estimate of  $x$ .

For each pixel  $i$ , let  $S \setminus \{i\}$  denote all other pixels in  $S$ . One of the most popular modeling assumptions is to consider the image  $x$  as being a realization of a Markov random field. This means that for all pixels  $i$  in  $S$ ,  $\mathbb{P}(x)$  satisfies  $\mathbb{P}(x_i|x_{S \setminus \{i\}}) = \mathbb{P}(x_i|x_{N(i)})$ ; that is, the conditional distribution of  $\mathbb{P}(x)$  depends only on the values of pixels in a subset  $N(i)$  of  $S \setminus \{i\}$ , called the *neighborhood* of pixel  $i$ . Another usual assumption is that, given  $\mathbf{X} = x$ , the  $\mathbf{Y}_i$  are conditionally independent and have the same conditional density function  $f(y_i|x_i)$  that depends only on  $x_i$ . Thus  $\mathcal{L}(y|x)$  can be written as the product  $\mathcal{L}(y|x) = \prod_{i \in S} f(y_i|x_i)$ .

Finding the MAP estimate under these assumptions can require heavy computation. A less computationally demanding method that provides a fast approximation to the MAP is the iterated conditional modes (ICM) algorithm (Besag 1986). The ICM algorithm is iterative. Given a current estimate  $\hat{x}$  of the image, a new one is computed by visiting each pixel in turn. At pixel  $i$ , the current value there is replaced by the value that maximizes the conditional density

$$\mathbb{P}(x_i|\hat{x}_{S \setminus \{i\}}, y), \quad (1)$$

given all other current pixel values  $\hat{x}_{S \setminus \{i\}}$  and the fixed observation  $y$ . This choice is motivated by the following equality, which holds for any pixel  $i$ :

$$\mathbb{P}(x|y) = \mathbb{P}(x_i|x_{S \setminus \{i\}}, y)\mathbb{P}(x_{S \setminus \{i\}}|y).$$

When pixels are updated sequentially, choosing values that maximize the conditional probability  $\mathbb{P}(x_i|x_{S \setminus \{i\}}, y)$  increases the posterior density  $\mathbb{P}(x|y)$  and ensures the convergence to a local maximum of  $\mathbb{P}(x|y)$ .

Under the previous modeling assumptions, maximizing the conditional density (1) is equivalent to maximizing

$$f(y_i|x_i)\mathbb{P}(x_i|\hat{x}_{N(i)}), \quad (2)$$

because only the dependence on  $x_i$  is relevant for the maximization. For unordered-color images, we focus, in Sections 3.1 and 3.2, on models simple enough to enable this maximization to be done explicitly. We show that for binary images the algorithm can be formulated using a morphological terminology.

## 2.2 Binary Mathematical Morphology

Mathematical morphology was first introduced as a tool for investigating geometric structure in binary images. In this context, binary images are usually viewed as subsets of a two-dimensional space, usually the two-dimensional discrete plane  $\mathbb{Z}^2$  or some finite subset  $S$  of it (the pixels) or, equivalently, as mappings from this set of pixels to  $\{0, 1\}$ . Geometric information can be extracted from a binary image by probing it with a small shape known as the structuring element. This element is a subset of  $\mathbb{Z}^2$ . To make it more similar to neighborhood structures in a Markov random field setting, it is assumed to contain the origin  $(0, 0)$  and to be symmetric. Note that this also simplifies some of the following definitions. Probably the most commonly used example of such an element is the  $3 \times 3$  square consisting of nine pixels.

Let  $I$  be an image and let  $B$  be a symmetric structuring element. For each pixel  $i \in S$ , let  $B(i)$  be the translation of  $B$  by  $i$ .  $B(i) = \{i + j, j \in B\}$ . The neighborhood  $N(i)$  of a pixel  $i$  is thus the translation by  $i$  of a symmetric structuring element  $N$ . A typical  $N$  would be the set of eight pixels in a  $3 \times 3$  square when the center of the square is not included.

The most primitive morphological operators are erosion and dilation. They are defined as

$$I \ominus B = \{i \in S, B(i) \subseteq I\}$$

and

$$I \oplus B = \{i \in S, B(i) \cap I \neq \emptyset\}.$$

A pixel  $i$  belongs to  $I$  eroded by  $B$  if  $B(i)$  is totally contained within  $I$ , whereas for pixel  $i$  to be in the dilation of  $I$  by  $B$ , it is enough that one pixel of  $B(i)$  belongs to  $I$ .

Erosion and dilation are dual notions. The so-called duality principle plays an important role in mathematical morphology. The dual,  $\psi^*$ , of a morphological operator  $\psi$  is defined by  $\psi^*(I) = (\psi(I^c))^c$  for all  $I \subset \mathbb{Z}^2$ , where  $I^c$  represents the complement of  $I$ . The erosion of the background of an image is equivalent to the dual dilation of its foreground. When an operator is equal to its dual, it is said to be self-dual. Self-dual operators treat the background and foreground of an image identically, and thus may be desirable when no a priori information is available on what is foreground and what is background.

When the intention is to remove noise from an image, another desirable property is idempotence. An operator  $\psi$  is said to be idempotent when  $\psi(\psi(I)) = \psi(I)$  for all  $I \subset \mathbb{Z}^2$ .

Erosion and dilation are not idempotent, but they can be combined into two idempotent operators called opening and closing. An opening is an erosion followed by a dilation,

$$I \circ B = (I \ominus B) \oplus B.$$

Its effect is roughly to delete small isolated parts and remove thin filaments of an image. A closing is a dilation followed by an erosion,

$$I \bullet B = (I \oplus B) \ominus B.$$

A closing is an opening of the image background. Opening and closing are dual notions in the sense that  $I \bullet B = (I^c \circ B)^c$ .

Openings and closings are the morphological operators commonly used to clean noisy images. They are based on erosions and dilations. The latter can be further generalized. They are particular cases of weighted rank operators as defined by Heijmans (1994). Let  $B$  be a structuring element with  $m$  points and let  $I_j$  denote the value (0 or 1) at pixel  $j$  when the image  $I$  is associated with a mapping from  $S$  to  $\{0, 1\}$ ; that is,

$$I_j = \begin{cases} 1 & \text{if } j \in I \\ 0 & \text{otherwise.} \end{cases}$$

Let  $W = \{w_1, w_2, \dots, w_m\}$  be the weights  $w_i$  associated with each pixel  $i$  in  $B$  and let  $r$  be a threshold or rank for  $w_1, \dots, w_m, r \in \mathbb{Z}$ . The weighted rank operator,  $\rho_{B,W,r}$ , is defined by

$$\rho_{B,W,r}(I) = \left\{ i \in S, \sum_{j \in B(i)} w_j I_j \geq r \right\}. \quad (3)$$

If the weights are positive, then such an operator is increasing (with respect to set inclusion). The negative of  $\rho_{B,W,r}$  is the weighted rank operator  $\rho_{B,W,r'}$  with  $r' = \sum_{i=1}^m w_i + 1 - r$ . It follows that  $\rho_{B,W,r}$  is self-dual if and only if  $2r = \sum_{i=1}^m w_i + 1$ . In that case,  $\rho_{B,W,r}$  is called a weighted median operator.

If  $w_i = 1$  for all  $i$  and  $1 \leq r \leq m$ , then  $\rho_{B,W,r}$  is called a rank operator and is simply denoted by  $\rho_{B,r}$ . For any two operators  $\psi_1$  and  $\psi_2$ , let  $\psi_1 \leq \psi_2$  denote the situation where  $\psi_1(I) \subset \psi_2(I)$  for every  $I \subset \mathbb{Z}^2$ . Then we have  $\rho_{B,m} \leq \rho_{B,m-1} \leq \dots \leq \rho_{B,1}$ . The operators  $\rho_{B,m}$  and  $\rho_{B,1}$  are erosion and dilation by  $B$ . More generally, rank operators can be decomposed as finite unions of erosions or intersections of dilations. For instance, we have  $\rho_{B,r}(I) = \cup_{B_0 \in \mathcal{V}_0} (I \ominus B_0)$ , where  $\mathcal{V}_0 = \{B_0 \subset B, |B_0| = r\}$ . Thus the rank operators are morphological operators in the sense of Matheron (1975) and Serra (1982). If  $m$  is odd and  $r = (m+1)/2$ , then  $\rho_{B,r}$  is self-dual and is usually referred to as the median operator. It has interesting cleaning capabilities and is sometimes combined with openings and closings to filter noisy images.

These rank operators are the ones that appear in the formulation (10) of ICM in the next section. They appear for different structuring elements, depending on the neighborhood structure chosen in the Bayesian analysis.

## 3. BAYESIAN MORPHOLOGY

In this section we first specify the ICM algorithm for some simple models. We show in Section 3.1 that for binary images, the ICM estimate of the true pixel [update rule (2)] is equivalent to the application of a mathematical morphology rank operator. When the noise and model parameters are known, ICM can be seen as a succession of rank operators whose ranks depend on the known parameters; see (10). When the noise and model parameters

are not known, a natural approach is to consider the unsupervised version of ICM, which consists of alternating between parameter estimation and restoration (see Sec. 4). One advantage of such a mathematical morphology formulation of the restoration step [update rule (10)] is to reveal the existence of insensitivity conditions for the parameters. This means that the final restoration is not sensitive to the precise values of the noise and model parameters. This is a key observation that we use to reduce the complexity of the estimation step in traditional unsupervised ICM and to save much computation time (see Theorem 2). We call the resulting algorithm and its extension to unordered-color images (Sec. 3.2) *Bayesian morphology*. When performed on unordered-color images, it is equivalent to ICM in the sense that the final restoration or classification is the same. In this case, it differs from ICM essentially in how the parameter estimation step is carried out. According to the insensitivity conditions, point estimates need not be computed.

### 3.1 Binary Images and Insensitivity Conditions in Iterated Conditional Modes

In the case of binary images,  $x_i \in \{0, 1\}$  and  $y_i \in \{0, 1\}$  for all pixels  $i$ . A commonly used prior distribution for the true image  $X$  is the attractive isotropic Ising model (in fact, the two-color Potts model),

$$\mathbb{P}(x) = Z(\beta)^{-1} \exp(\beta v(x)), \quad (4)$$

where

$$v(x) = \sum_{i \sim j} \delta(x_i, x_j) \quad (5)$$

is the number of pairs of neighboring pixels having the same color in  $x$ . In the foregoing sum,  $i \sim j$  denotes the statement that the pixels  $i$  and  $j$  are neighbors and  $\delta(x_i, x_j)$  refers to the Kronecker delta function, equal to 1 if  $x_i$  and  $x_j$  are the same and to 0 otherwise. The quantity  $Z(\beta)$  is the normalizing constant, or partition function,

$$Z(\beta) = \sum_x \exp(\beta v(x)). \quad (6)$$

This function is usually difficult to compute because of the intractably large number of terms in the summation. The conditional distributions of  $\mathbb{P}(x)$  have the simple form

$$\mathbb{P}(x_i | x_{S \setminus \{i\}}) \propto \exp(\beta u_i(x_i)), \quad (7)$$

where

$$u_i(x_i) = \sum_{j \in N(i)} \delta(x_i, x_j) \quad (8)$$

is the number of neighbors of pixel  $i$  having color  $x_i$ . The model depends on a parameter  $\beta$  that is taken to be positive, reflecting the assumption that neighboring pixels tend to be of the same color.

The true images are then assumed to be degraded by a region-dependent flip-flop, or channel transmission noise characterized by the two parameters  $p_{01}$  and  $p_{10}$ , where

$p_{01} = \mathbb{P}(y_i = 1 | x_i = 0)$  and  $p_{10} = \mathbb{P}(y_i = 0 | x_i = 1)$ . We assume, without loss of generality, that  $p_{01}$  and  $p_{10}$  belong to the open interval  $(0, 1/2)$ . The  $y_i$  are assumed to be conditionally independent and the likelihood is  $\mathcal{L}(x|y) = \prod_{i \in S} f(y_i | x_i)$ , where  $f(y_i | 1) = (1 - p_{10})^{y_i} (p_{10})^{1-y_i}$  and  $f(y_i | 0) = (p_{01})^{y_i} (1 - p_{01})^{1-y_i}$ .

For these noise and image models, the update rule (2) in ICM can be written explicitly. In what follows,  $\lceil \cdot \rceil$  and  $\lfloor \cdot \rfloor$  denote the floor and the ceiling functions.

**Theorem 1.** For an Ising model with region-dependent flip-flop noise, the current ICM estimate of the true image at pixel  $i$  is updated by changing  $\hat{x}_i$  to  $x_i^*$  according to the rule

$$x_i^* = \begin{cases} 1 & \text{if } u_i(1) - u_i(0) \geq 2w_1 \\ 0 & \text{if } u_i(1) - u_i(0) < -2w_0 \\ y_i & \text{if } -2w_0 \leq u_i(1) - u_i(0) < 2w_1, \end{cases} \quad (9)$$

where  $w_0$  and  $w_1$  are positive integers that depend on the noise and model parameters  $p_{01}$ ,  $p_{10}$ , and  $\beta$ , namely

$$w_0 = \left\lceil \frac{1}{2\beta} \log \left( \frac{1 - p_{10}}{p_{01}} \right) \right\rceil$$

and

$$w_1 = \left\lceil \frac{1}{2\beta} \log \left( \frac{1 - p_{01}}{p_{10}} \right) \right\rceil.$$

Note that  $u_i(1) + u_i(0) = |N(i)| = m$ , so that  $u_i(1) - u_i(0) = 2u_i(1) - |N(i)|$  is even for every symmetric neighborhood  $N(i)$ , where  $|N(i)|$  is the number of elements in  $N(i)$ . For binary images, we have  $u_i(1) = \sum_{j \in N(i)} x_j$ , and an equivalent formulation of (9) can be given in terms of the rank operators defined in (3):

$$x_i^* = \begin{cases} \lfloor \rho_{N, r_0}(\hat{x}) \rfloor_i & \text{if } y_i = 0 \\ \lceil \rho_{N, r_1}(\hat{x}) \rceil_i & \text{if } y_i = 1. \end{cases} \quad (10)$$

where  $r_0 = (m/2) + w_1$  and  $r_1 = (m/2) - w_0$  and where  $[z]_i$  is the value of the image  $z$  at pixel  $i$ . A shorter way to write (10) is  $x_i^* = \lceil \rho_{N, r_i}(\hat{x}) \rceil_i$ , where  $r_i = (m/2) + w_1 - y_i(w_0 + w_1)$ .

The update rule (9) depends on the parameters  $p_{01}$ ,  $p_{10}$  and  $\beta$  only through the values of  $w_0$  and  $w_1$ . When these integers are known, each pixel can be updated easily by applying the rule (9) or, equivalently, the rank operators  $\rho_{N, r_0}$  or  $\rho_{N, r_1}$ . In the general case,  $p_{01}$ ,  $p_{10}$  and  $\beta$  are unknown and so are  $w_0$  and  $w_1$ . However, we have the following result.

**Theorem 2.** If there exist integers  $k_0$  and  $k_1$  such that  $p_{01}$ ,  $p_{10}$ , and  $\beta$  satisfy

$$\frac{1}{2(k_0 + 1)} \log \left( \frac{1 - p_{10}}{p_{01}} \right) < \beta \leq \frac{1}{2k_0} \log \left( \frac{1 - p_{10}}{p_{01}} \right) \quad (11)$$

and

$$\frac{1}{2k_1} \log \left( \frac{1 - p_{01}}{p_{10}} \right) \leq \beta < \frac{1}{2(k_1 - 1)} \log \left( \frac{1 - p_{01}}{p_{10}} \right). \quad (12)$$

then for all of these values of  $p_{01}$ ,  $p_{10}$ , and  $\beta$ ,  $w_0$  and  $w_1$  are equal to  $k_0$  and  $k_1$ . These conditions can be equivalently formulated in terms of  $p_{01}$  and  $p_{11} = 1 - p_{10}$ :

$$p_{01}a^{k_0} \leq p_{11} < p_{01}a^{k_0+1} \quad (13)$$

and

$$p_{01} \frac{1}{a^{k_1-1}} + 1 - \frac{1}{a^{k_1-1}} < p_{11} \leq p_{01} \frac{1}{a^{k_1}} + 1 - \frac{1}{a^{k_1}}. \quad (14)$$

where  $a = \exp(2/\beta)$ .

It follows that the update rule (9) does not depend on the exact values of  $p_{01}$ ,  $p_{10}$ , and  $\beta$ , but rather on how they are related to each other. We refer to (11) and (12) [or (13) and (14)] as the *insensitivity conditions*. Figure 1 shows the sets of values of  $p_{01}$  and  $p_{11}$  within which  $w_0$  and  $w_1$  are constant. Estimating  $w_0$  and  $w_1$  then consists of finding  $k_0$  and  $k_1$  such that the insensitivity conditions hold. We can restrict our search to values of  $k_0$  in  $\{0, 1, \dots, |N(i)|/2 - 1\}$  and  $k_1$  in  $\{1, \dots, |N(i)|/2\}$ . Indeed, if  $w_1 \geq |N(i)|/2 + 1$ , then  $y_i = 0$  automatically implies that  $x_i^* = y_i$ . A particular case occurs when  $w_1 = 1 + w_0$ . For these values,  $\rho_{N, r_1}$  and  $\rho_{N, r_1}$  are dual operators. Note that this is satisfied when  $p_{01} = p_{10}$ ; that is, when foreground and background noise are treated identically. Another particular case is  $w_1 = 1 - w_0$ , which actually corresponds to  $w_0 = 0$  and  $w_1 = 1$ . This occurs when

$$\beta > \frac{1}{2} \log \left( \frac{1 - p_{10}}{p_{01}} \right) \quad (15)$$

and

$$\beta \geq \frac{1}{2} \log \left( \frac{1 - p_{01}}{p_{10}} \right). \quad (16)$$

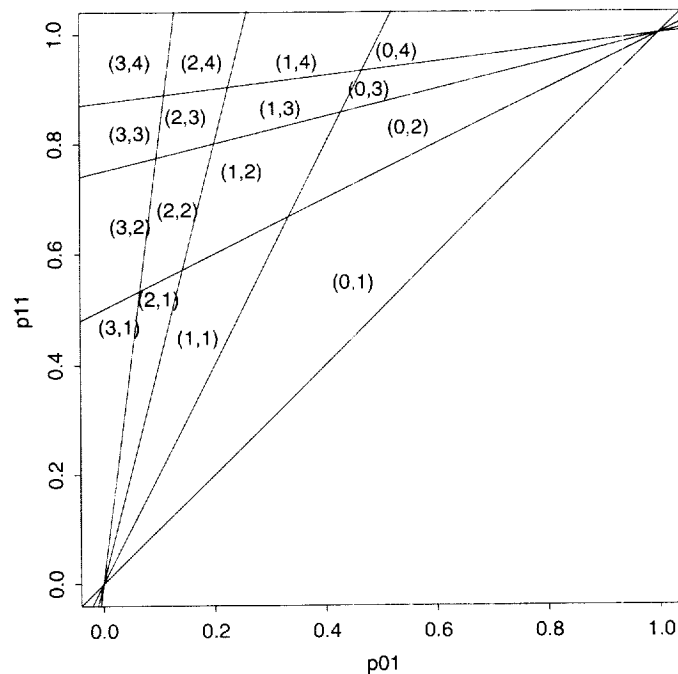


Figure 1. Insensitivity Conditions in Terms of  $p_{01}$  and  $p_{11}$  for an Eight-Pixel Neighborhood With  $\beta = .35$ . The lines delimit regions where  $w_0$  and  $w_1$  are constant. Their respective values are shown in parentheses. For example, in the largest triangle region, notation (0, 1) means that for all values of  $p_{01}$  and  $p_{11}$  lying in this region,  $w_0 = 0$  and  $w_1 = 1$ .

leading to the following theorem.

**Theorem 3.** If  $p_{01}$ ,  $p_{10}$ ,  $\beta$  satisfy conditions (15) and (16), then the update rule (9) does not involve any parameters. It becomes

$$x_i^* = \begin{cases} 1 & \text{if } u_i(1) > u_i(0) \\ 0 & \text{if } u_i(1) < u_i(0) \\ y_i & \text{if } u_i(1) = u_i(0). \end{cases} \quad (17)$$

This corresponds to the blind restoration proposed by Zhang, Shirazi, and Noda (1996). Other blind restorations can be derived by assuming different values for  $w_0$  and  $w_1$ . They may be more appropriate, depending on the true parameter values (see Sec. 5). However, update rule (17) consists of applying the majority rule and may be viewed as a reasonable first choice of blind restoration for many images. Note that this choice corresponds to the largest region in Figure 1.

Our alternative to arbitrary blind restoration involves estimating  $w_0$  and  $w_1$ . In Section 4 we show that this turns out to be much easier than computing point estimates for  $p_{01}$ ,  $p_{10}$ , and  $\beta$ . But first, we consider similar developments for color images.

### 3.2 Unordered-Color Images

A widely used model for images with  $C$  unordered exchangeable colors is the Potts model defined here. Such a model is adapted to image segmentation or classification, where the goal is to assign to each pixel of the observed image a label (or color) indicating the pixel's class. The standard nearest-neighbor Potts model is defined by the joint distribution

$$\mathbb{P}(x) = Z(\beta)^{-1} \exp(\beta v(x)). \quad (18)$$

where the expressions (5), (6), (7), and (8) remain valid, keeping in mind that they may refer to more than two colors. Note that in the infinite size limit, this model has a phase transition at  $\beta_{\text{crit}} = \log(1 + \sqrt{C})$  when there are four neighbors (Georgii 1988).

To derive insensitivity conditions as in Section 3.1, the key step is to formulate the update rule in ICM so that the discrete nature of the images can be exploited in a simple way. For that reason, we restrict attention to the following independent noise model:

$$f(y_i|x_i) = \begin{cases} 1 - p & \text{if } y_i = x_i \\ \frac{p}{C-1} & \text{otherwise.} \end{cases} \quad (19)$$

This corresponds to transmission with channel noise. A good transmission is assumed to be the most probable, which means that  $C(1 - p) > 1$ . More general models are possible, but they lead to more complex update rules. For instance, a region-dependent degradation where  $p$  in (19) would be replaced by values  $p_{x_i}$  that may depend on  $x_i$  could be considered. This would better generalize Section 3.1, but formulating it properly would require the estimation of  $(C - 1)(3C - 2)/2$  integers instead of the two,  $w_0$  and  $w_1$ , in (9). Adopting the foregoing simple noise model

leads to a formulation of ICM update rule very similar to that in the binary image case. Let  $\hat{x}$  be the current restoration as in Section 3.1.

**Theorem 4.** For a Potts model with channel noise, ICM works as follows. When at pixel  $i$ , the current value  $\hat{x}_i$  is changed to  $x_i^*$  according to the procedure below:

- Find the color that is taken most often by the neighbors of pixel  $i$  in  $\hat{x}$ ; that is, find  $c$  in  $\{\hat{x}_j, j \in N(i)\}$  such that  $u_i(c)$  is maximized.
- Then, update pixel  $i$ :

$$x_i^* = \begin{cases} c & \text{if } u_i(c) - u_i(y_i) \geq w \\ y_i & \text{otherwise,} \end{cases} \quad (20)$$

where  $w$  is a positive integer that depends on the parameters,

$$w = \left\lceil \frac{1}{\beta} \log \left( \frac{(1-p)(C-1)}{p} \right) \right\rceil.$$

The update rule (20) depends on  $\beta$  and  $p$  only through the value of  $w$ . This leads to the following insensitivity conditions.

**Theorem 5.** For the Potts model with channel noise, if there exists an integer  $k$  such that  $\beta$  and  $p$  satisfy

$$k-1 < \frac{1}{\beta} \log \left( \frac{(1-p)(C-1)}{p} \right) \leq k, \quad (21)$$

or, equivalently,

$$\begin{aligned} \frac{1}{k} \log \left( \frac{(1-p)(C-1)}{p} \right) \\ \leq \beta < \frac{1}{k-1} \log \left( \frac{(1-p)(C-1)}{p} \right), \end{aligned} \quad (22)$$

or in terms of  $p$ ,

$$\begin{aligned} \frac{1}{1 + (C-1)^{-1} \exp(\beta k)} \\ \leq p < \frac{1}{1 + (C-1)^{-1} \exp(\beta(k-1))}. \end{aligned} \quad (23)$$

then  $w$  is equal to  $k$ , and the ICM update rule (20) does not depend on the exact values of  $\beta$  and  $p$ .

Estimating  $w$  then reduces to finding  $k$  such that one of the foregoing equivalent expressions is satisfied. In Section 4 we propose a way to do so, avoiding the need for point estimation.

#### 4. ONLINE PARAMETER ESTIMATION

When the model and noise parameters are unknown, a natural approach to unsupervised restoration is first to estimate the parameters and then to estimate the true unknown scene  $x$  (see Sec. 2.1) given the parameter estimates. This is usually done iteratively by iterating between parameter estimation and restoration, following the general procedure proposed by Besag (1986). In most cases, estimating the

noise parameters does not present a problem (maximum likelihood estimators are usually available in closed form), and the main difficulty arises in the estimation of the parameters of the model for the true scene (or "prior" model). Maximum likelihood estimation is usually intractable, except maybe in some cases (see Goutsias 1991), because of the practical impossibility of computing the partition function. In practice, estimation is based on approximations such as maximum pseudolikelihood (Besag 1975). If the Potts model is "true," then this may lead to inaccurate estimators, especially when the dependency is high (Geyer 1991), but for actual images it may yield better restorations, given the often unrealistic *global* behavior of the Potts model (Besag 1986).

In our setting, however, maximum likelihood estimation appears to require a reasonable amount of computation. The idea is to take advantage of the insensitivity conditions given in Sections 3.1 and 3.2. They allow one to find the restoration based on the maximum likelihood estimate without ever actually finding the maximum likelihood estimator explicitly, a fact that leads to great computational savings.

Our algorithms are based on estimation criteria. An estimation criterion is a function that measures the quality of a parameter. We let  $\beta$  denote such a parameter and  $\hat{\beta}$  denote the value at which such a function is maximized, assuming that such a maximum exists. More generally,  $\hat{\beta}$  may be an estimator of a parameter of interest, and we call an estimation criterion any monotone function  $f$  such that  $f(\hat{\beta})$  is known (although  $\hat{\beta}$  is not necessarily known) and  $f(\beta)$  is computable for any given value of  $\beta$ . Typically, if  $F$  is a concave function with maximum at  $\hat{\beta}$ , then its derivative  $(dF/d\beta)$  is decreasing and equal to 0 at  $\hat{\beta}$ . If this derivative is computable for given values of  $\beta$ , then  $f = (dF/d\beta)$  or  $f = -(dF/d\beta)$  can be termed an estimation criterion.

We use such functions to find  $w_0$  and  $w_1$  if the model is that of Section 3.1, and to find  $w$  if the model is that of Section 3.2. The two cases are similar, and we focus on the model of Section 3.2. The value of  $w$  is the integer  $k$  that satisfies (22), which for any increasing function  $f$  is equivalent to

$$\begin{aligned} f \left( \frac{1}{k} \log \left( \frac{(1-p)(C-1)}{p} \right) \right) \\ \leq f(\beta) < f \left( \frac{1}{k-1} \log \left( \frac{(1-p)(C-1)}{p} \right) \right). \end{aligned}$$

Therefore, if  $\hat{\beta}$  is an estimator of  $\beta$ , then a natural estimator of  $w, \hat{w}$ , satisfies

$$\begin{aligned} \frac{1}{\hat{w}} \log \left( \frac{(1-p)(C-1)}{p} \right) \\ \leq \hat{\beta} < \frac{1}{\hat{w}-1} \log \left( \frac{(1-p)(C-1)}{p} \right). \end{aligned}$$

Equivalently, if  $f$  is such that  $f(\hat{\beta})$  is equal to a known constant  $b$ , then  $\hat{w}$  satisfies

$$f\left(\frac{1}{\hat{w}} \log\left(\frac{(1-p)(C-1)}{p}\right)\right) \leq b < f\left(\frac{1}{\hat{w}-1} \log\left(\frac{(1-p)(C-1)}{p}\right)\right). \quad (24)$$

If  $f((1/k) \log((1-p)(C-1)/p))$  is known for different integer values  $k$ , then finding  $\hat{w}$  reduces to comparing real values, which is easier than computing  $\hat{\beta}$ . In earlier work (Forbes and Raftery 1997), we considered in detail the cases corresponding to maximum likelihood and maximum pseudolikelihood estimation for the standard Potts model (18). For maximum likelihood estimation, we showed that an appropriate function  $f$  and the corresponding value  $b$  are  $f(\beta) = \mathbb{E}_{\beta}[v(\mathbf{X})] = \sum_v v(u) \mathbb{P}(u)$ , which depends on  $\beta$  through  $\mathbb{P}$ , and  $b = \mathbb{E}_{\hat{\beta}}[v(\mathbf{X})] = v(x)$ , where  $\hat{\beta}$  is the maximum likelihood estimator of  $\beta$ .

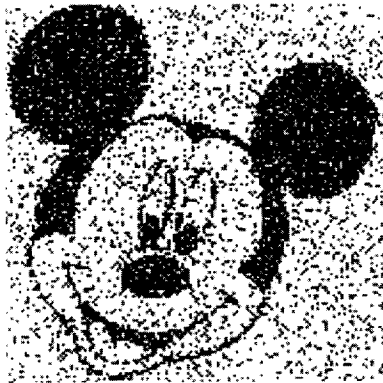
The exact computation of the foregoing expectations is intractable. However, estimates can be obtained by sampling the distribution  $\mathbb{P}(x)$  for the corresponding values of  $\beta$  and forming empirical averages. The required samples can be generated using Markov chain Monte Carlo.

This can be computationally demanding, but we were able to accelerate it greatly for the Potts model using the Swendsen–Wang algorithm (Swendsen and Wang 1987). Our algorithm requires only a small number of samples and evaluations. Other approaches that try to save on-line samplings include those of Descombes, Morris, and Zerubia (1996), Geyer (1991), and Geyer and Thompson (1992).

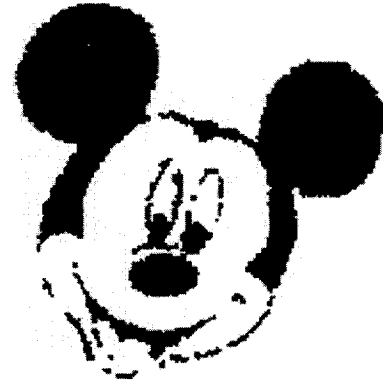
Pseudolikelihood estimation appears as a natural alternative to maximum likelihood, which is usually intractable in the standard Markov random field cases when point estimation of the parameters is required. The term “pseudolikelihood” was introduced by Besag (1975) to refer to the product of conditional probabilities,

$$\prod_{i \in S} \mathbb{P}(x_i | x_{S \setminus \{i\}}). \quad (25)$$

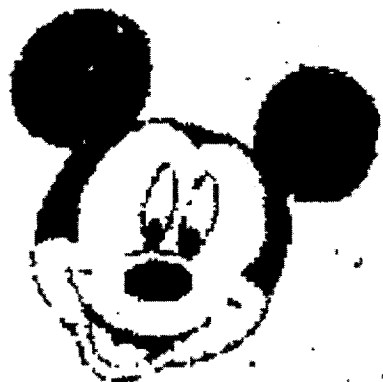
For the Potts model,  $\mathbb{P}(x_i | x_{S \setminus \{i\}}) = p_i(x_i) = Z_i(\beta)^{-1} \exp(\beta u_i(x_i))$ , where  $Z_i(\beta) = \sum_{c \in \{1, \dots, C\}} \exp(\beta u_i(c))$ . In this case an appropriate function  $f$  is  $f(\beta) = \sum_{i \in S} \mathbb{E}_{p_i}[u_i(\mathbf{X}_i)]$ , and the corresponding constant  $b$  is  $b = \sum_{i \in S} u_i(x_i) = 2v(x)$ . An advantage over maximum likelihood estimation is the possibility of computing  $\sum_{i \in S} \mathbb{E}_{p_i}[u_i(\mathbf{X}_i)]$  exactly.



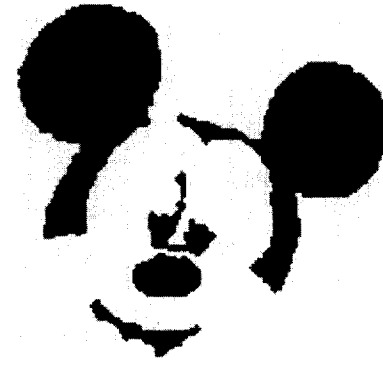
(a)



(b)



(c)



(d)

Figure 2. Degraded Mickey Image and Different Unsupervised Restorations. (a) Original image degraded with 5% channel noise. (b) Bayesian morphology based on a likelihood criterion. (c) Bayesian morphology based on a pseudolikelihood criterion. In (b) and (c), the initial estimate of the noise parameter  $\hat{p}_0$  was .35. (d) Blind restoration using simple majority rule.

## 5. EXPERIMENTS

### 5.1 Restoring Unordered-Color Images

We first consider pure restorations of unordered-color images. The steps of the Bayesian morphology algorithm are not listed here; more details and other images can be found in our earlier work (Forbes and Raftery 1997). Figure 2 shows a binary image degraded with 15% channel noise and different restorations: Bayesian morphology using the likelihood and pseudolikelihood criteria (see Sec. 4) and blind restoration using the simple majority vote (17), following Zhang et al. (1996).

The performance of our Bayesian morphology algorithm is the same as that of an unsupervised version of ICM. Table 1 gives the final estimates of  $p$  and  $w$ , the number of iterations before convergence and the number of calls to the function  $f$  used in (24). The number of times that the estimation criterion (function  $f$ ) is evaluated is relevant to the speed of the algorithm, especially for maximum likelihood, because such evaluations require online sampling and may slow the restoration procedure considerably. To initialize our procedure, we set the initial value of the noise parameter  $p$  to .35.

Note that for a two-color Potts model, the term  $(u_i(c) - u_i(y_i))$  in the update rule (20) is even. Therefore, an odd value of  $w$  and the even integer following it actually lead to the same updating. Thus, in this case the number of calls to  $f$  can be divided by 2. Although computationally unnecessary, the distinction is interesting when comparing maximum likelihood and maximum pseudolikelihood estimators of  $\beta$ , as a smaller value of  $w$  corresponds to a larger value of  $\beta$ . In Table 1 the pseudolikelihood criterion results in an estimate of  $w$  equal to 3, compared to 4 when a likelihood criterion is used. For binary images, those values of  $w$  correspond to the same updating of the current restoration, so that for the noisy image (a), likelihood and pseudolikelihood criteria lead to similar restorations (b) and (c). The restorations are different, however, because the first updating is different in each procedure. The fact that a pseudolikelihood criterion leads to a lower estimate of  $w$  is consistent with the empirical observation of Geyer and Thompson (1992) that maximum pseudolikelihood estimators tend to overestimate  $\beta$ . As illustrated in Figure 2, blind restoration performs badly. Too much detail is lost, and the error rate is higher.

The choice of estimation criterion may be important in this setting. Theoretical studies and empirical comparison of the maximum likelihood and maximum pseudolikelihood estimators for Markov random fields have been carried out by various authors. Comets and Gidas (1992) and Gidas

(1993) showed both the maximum likelihood and maximum pseudolikelihood estimators to be consistent. This does not necessarily say very much about their properties when used on finite lattices. Tjelmeland (1996) presented simulation experiments with maximum likelihood and maximum pseudolikelihood estimators for binary Markov random fields on moderately sized hexagonal lattices (2,883 to 30,603 pixels). The results indicate that both estimators give good results for the Ising model and for models with weak interactions between neighboring pixels. For models with strong interactions, the maximum pseudolikelihood estimator produces unsatisfactory estimates, whereas maximum likelihood estimator still gives reliable results. However, as Tjelmeland (1996) observed, estimated parameter values substantially different from the true values do not necessarily mean that the visual appearance of the corresponding realizations of the model differs from that of the true model. This is an important point in image analysis, where modeling per se may not be the primary goal.

In our setting, the parameter estimation step cannot be considered independently of the restoration step. The main advantage in using insensitivity conditions is to avoid the problematic computation of pointwise estimates. Therefore, our comparison of the estimation criteria must be based on the quality of the final restoration or segmentation. How to evaluate this quality depends on the task at hand. Also, when considering a visual criterion for assessing the quality of an estimator, the actual performance may be masked by the choice of the prior model. On one hand, more accurate parameter estimation (via maximum likelihood) allows more reliable comparisons of different priors. In particular, the Potts model and, more generally, models that involve only pairwise interactions (Descombes et al. 1996; Tjelmeland and Besag 1998) can be shown to not capture well the global characteristics of images. On the other hand, these models may perform surprisingly well in tasks such as restoration while performing poorly for other tasks (see Tjelmeland and Besag 1998). Descombes et al. (1996) showed cases where the restored images using the Potts model as a priori may still be noisy. A common trick for obtaining better restorations is to overregularize the solution by increasing  $\beta$ . In that sense, it is not surprising that a pseudolikelihood criterion may produce good results. Ideally, we recommend using accurate parameter estimation and more realistic priors, such as the higher-order Markov random fields described by Descombes, Mangin, Pechersky, and Sigelle (1995) and Tjelmeland and Besag (1998). But this is much more demanding in terms of computation

Table 1. Results for Figure 2 (Mickey Image With 15% Channel Noise)

Image	Iterations	Calls to $f$	Final $k$	Final $p$	Error rate
(a) 15% channel noise					14.9%
(b) Likelihood criterion ( $\hat{p}_0 = .35$ )	7	30	4	14.4%	1.8%
(c) Pseudo-likelihood criterion ( $\hat{p}_0 = .35$ )	9	30	3	13.9%	1.8%
(d) Blind restoration ( $w = 1$ )	20		1	16.4%	3.2%

NOTE:  $f$ ,  $k$ , and  $p$  are defined in the text.



and time, so that in practice the Potts model may still be preferred by users.

## 5.2 Segmenting Gray-Scale and Multidimensional Images

In the previous cases, the observed and unobserved images were of the same type. Often, however, the image to be restored consists of unordered colors (classes), but the observations are usually ordered real values (measurements). The ICM algorithm can be used for such restorations, assuming a different noise model (Besag, York, and Mollié 1991), but our use of the insensitivity conditions cannot be extended efficiently for this model. We believe, however, that they can still be used to obtain acceptable segmentations rapidly.

A natural idea when dealing with more general images (possibly multidimensional data) is to first derive an initial classification using simple and fast procedures, such as the maximum likelihood classifier [ $\hat{x}_i$  is chosen to maximize  $f(y_i|x_i)$  at each pixel  $i$  separately]. These procedures do not take spatial information into account and may result in an unacceptably large number of misclassified pixels. Therefore, a better classification can be computed by assuming the initial classification to be a noisy version of the final one according to the model in Section 3.2. The performance of such an alternative depends on the quality of the initial restoration. It cannot be expected to perform quite as well as algorithms that do not lose track of the original (e.g., continuous, gray-level) data, but in our experiments it performs similarly and can be much faster.

The maximum likelihood classifier requires that the user either know in advance or be prepared to specify the parameters that define  $f(y_i|x_i)$ . Alternatively, *representative* training data must be available, consisting of pixels whose class is known. These conditions will often not be met. Here we used a simple alternative, *marginal mixture EM segmentation*, which yields a reasonable initial classification without requiring either specialized user knowledge or training data. The marginal distribution of gray-scale pixel intensities is assumed to be of the form of a finite mixture of distributions. More details of this procedure can be found in our earlier work (Forbes and Raftery 1997).

For multispectral images, the same approach as for gray-scale images can be used, in principle. An additional difficulty arises, however—the important problem of initializing the EM algorithm. We have found that agglomerative hierarchical *model-based clustering* (Banfield and Raftery 1993; Celeux and Govaert 1995) provides a sensible way of doing this (see Dasgupta and Raftery 1998). This can be done using the mclust software, which is part of S-PLUS, and can also be obtained at <http://lib.stat.cmu.edu/general/mclust> (Fortran version), or <http://lib.stat.cmu.edu/S/mclust> (S version).

For standard-sized images, such as  $256 \times 256$  or  $512 \times 512$ , this clustering can be computationally expensive, but clustering on the basis of a subsample of pixels is fast and often works well (Banfield and Raftery 1993). The resulting parameter estimates for the mixture model can be used

to initialize the EM algorithm, or to provide an initial classification directly via discriminant analysis (Banfield and Raftery 1993; Bensmail and Celeux 1996).

Another way of getting a fast first classification via marginal mixture EM segmentation without first subsampling the pixels has been described by Posse (1998). This method involves combining a minimum spanning tree algorithm with a classification procedure so that a large number of points (pixels) can be handled.

## 5.3 Example: Gray-Level Image of a Dog Lung

Figure 3(a) is a gray-level image of a dog lung. The aim here was to distinguish the lung from the rest of the image to measure the heterogeneity of the tissue in the region of interest. Only pixels in this delimited area are then considered to compute a heterogeneity measure, such as a coefficient of variation. The EM algorithm was used to compute the three-component segmentation (b), which is a good initial segmentation apart from some misclassified pixels. The final segmentations using standard ICM and Bayesian morphology are shown in (c) and (d).

Although perhaps visually more pleasing, the standard ICM segmentation (c) is slightly too smooth for the specific purpose of the study, and the Bayesian morphology segmentation (d) may be preferred. Note that this observation is consistent with the corresponding estimates  $\hat{\beta}$  of  $\beta$ . In the Bayesian morphology case, only bounds are available for  $\hat{\beta}$  ( $1.05 \leq \hat{\beta} < 1.40$ ). For ICM, the estimate is  $\hat{\beta} = 1.44$ ; this is higher than the higher bound, confirming that the subsequent restoration may be smoother. The Bayesian morphology segmentation represents the nonlung area inside the lung as an “island,” whereas the ICM segmentation connects it to the area outside the lung; the researchers preferred the Bayesian morphology solution in this respect. Also, standard ICM produces a more jagged restoration of the outside circle than Bayesian morphology, and again in this respect our external knowledge indicates the Bayesian morphology solution to be more faithful to reality. In addition, Bayesian morphology was 3.5 times faster than ICM.

## 5.4 Example: Precipitation Climatology

Input data are data for a global precipitation climatology produced at the Joint Institute for the Study of the Atmosphere and Ocean (available at [http://www.tao.atmos.washington.edu/legates\\_msu](http://www.tao.atmos.washington.edu/legates_msu)). The spatial resolution of this climatology is 2.5 degrees in latitude and in longitude, which leads to a set of 12  $144 \times 72$  maps representing stations or points (pixels) at which monthly average precipitation (in mm) has been recorded or extrapolated, for each individual calendar month. Figure 4 shows such a map for the month of January.

Possible goals of classifying these data into a small number of components include building climatic regionalizations to show climatic variability and defining local forecast zones consisting of groups of stations, each of which would be considered a single locale for forecasting purposes, thus reducing the total number of stations. Fovell

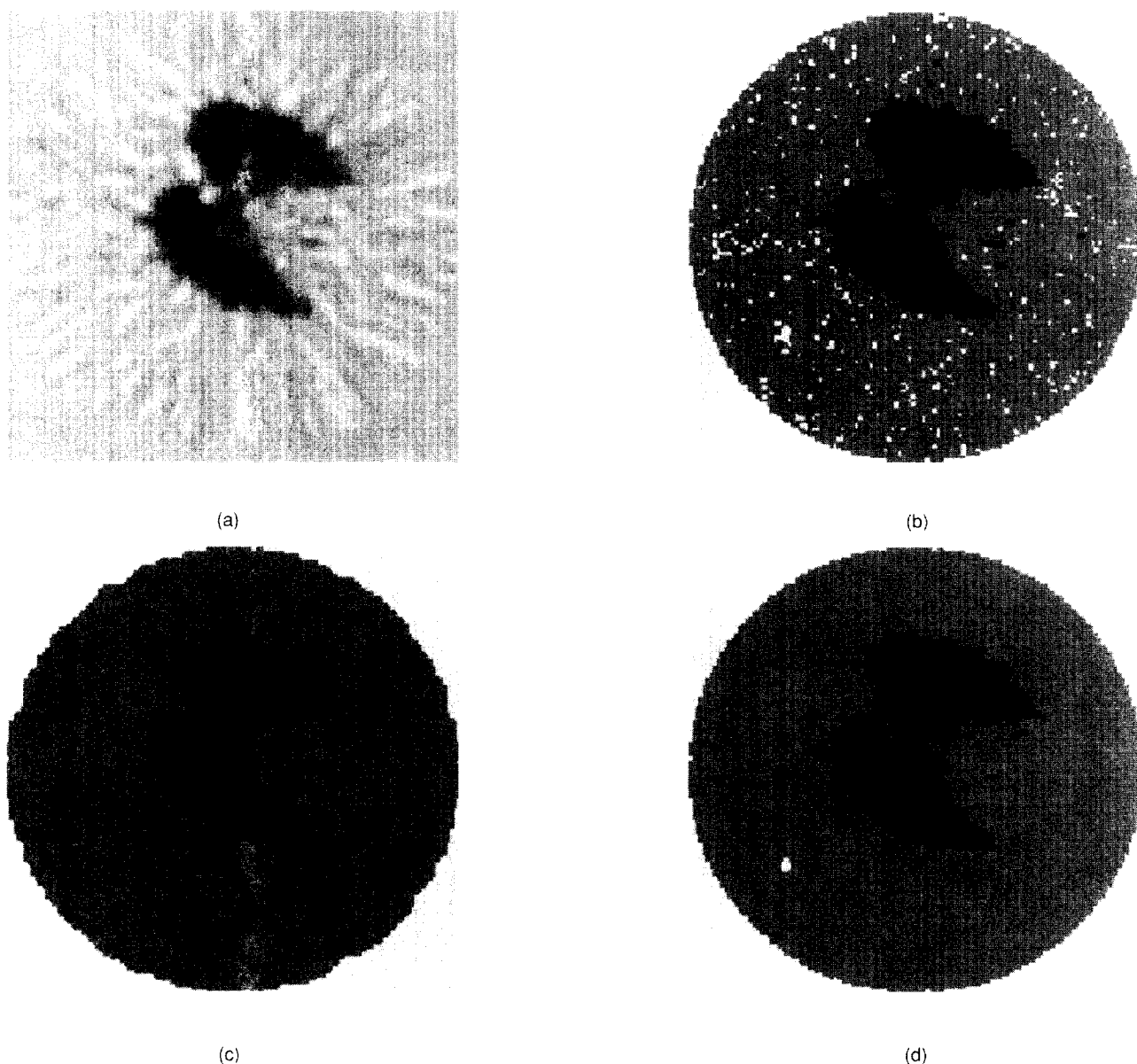


Figure 3. A Gray-Level Image of a Dog Lung, and Different Unsupervised Segmentations. (a) Original grey-level image; (b) initial three-component segmentation using the marginal mixture model EM method; (c) standard ICM segmentation, starting from (b); (d) Bayesian morphology segmentation, modeling the initial segmentation (b) as being degraded by channel noise.

(1997) has provided more background and considered similar data for the purpose of delineating climate zones of the conterminous United States. That study used standard clustering techniques that do not take into account spatial location and dependence. These techniques have the drawback of producing small separate entities that are not climatologically meaningful. Using ICM or Bayesian morphology to classify these data has the advantage of producing more spatially cohesive regionalizations. Small isolated regions are removed by automatically reassigning the stations (pixels) located in them, reducing the spatial fragmentation of the classifications.

We computed six-component classifications following a suggestion of Fovell (1997). As these data are far from normally distributed, a nonlinear transform was first applied; the power .25 of each record was taken. A fast first segmen-

tation of the  $144 \times 72$  12-band image was then obtained using the technique described by Posse (1998). Figure 5 shows this classification after applying Bayesian morphology with an initial value of  $\hat{w}$  set to 1. The Bayesian morphology segmentation ( $1.15 < \hat{\beta} < 1.53$ ) appears too fragmented in some regions, whereas the ICM segmentation ( $\hat{\beta} = 1.77$ ) appears too smooth. In the latter, significant regions are removed near the islands of Madagascar and New Zealand, for instance. Another advantage of Bayesian morphology is that for this 12-band image, it was 13 times faster than ICM.

Note that, depending on the goal of the analysis, the data may be preprocessed differently. If the goal is to construct local forecast zones, then it may be judged prudent to standardize the records to eliminate level (mean) and seasonality (variance) distinctions. In the present application, we were

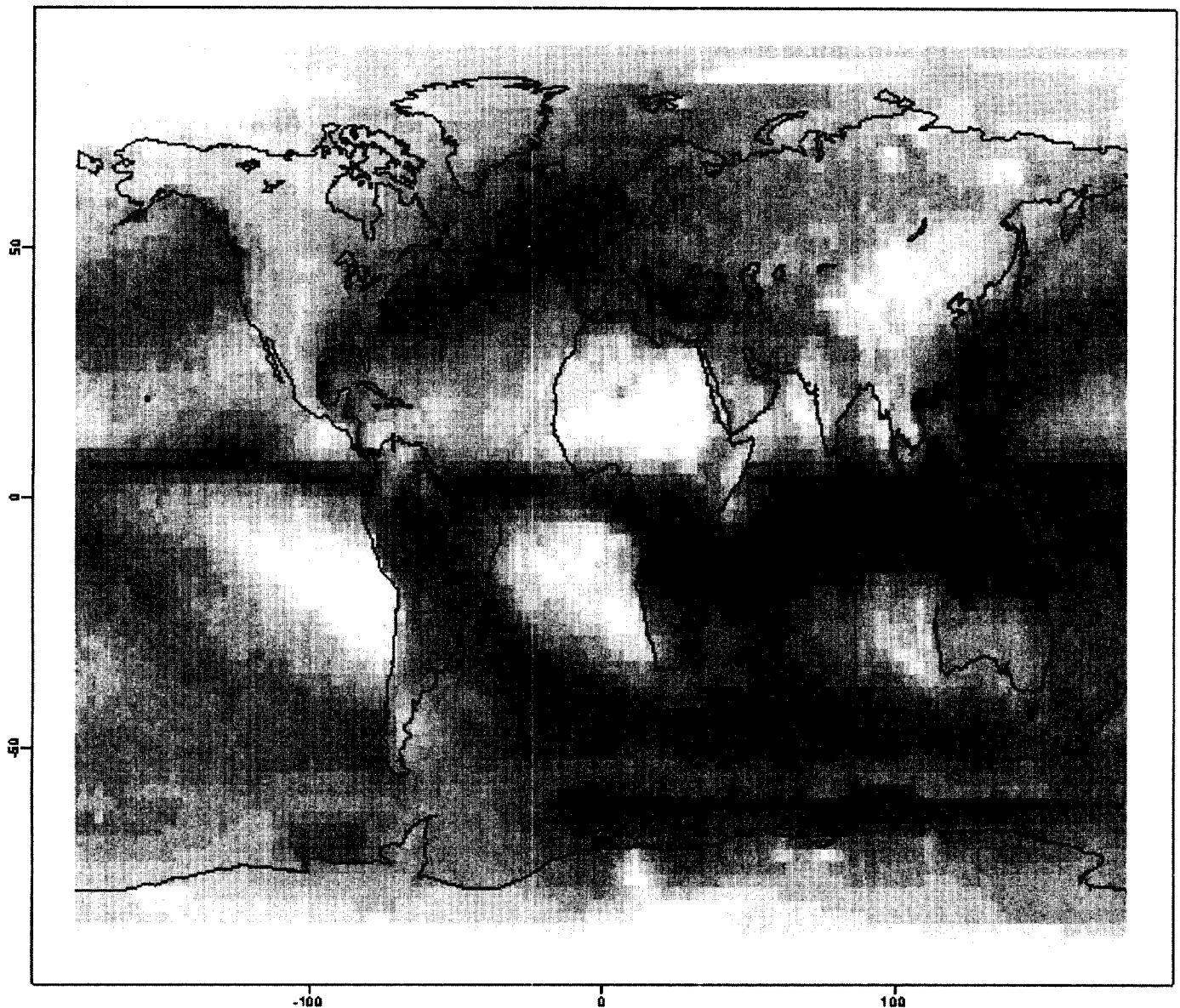


Figure 4. Monthly Average Precipitation (mm) for the Month of January. The spatial resolution is 2.5 degrees in each of latitude and longitude and results in a  $144 \times 72$  image.

more concerned with the construction of climatic zones for which the level and seasonality components are useful information. Time series can be computed by averaging the data for the members in each class of Figure 5 (see fig. 17 in Forbes and Raftery 1997). In this classification, class 1 is represented in white class 6, in black. Classes 1 and 2 correspond to dry regions with different seasonalities. Class 6 corresponds to wet areas with light seasonal variations. Class 3 includes regions with high variability and dry summer climates, and class 5 includes continental interiors that generally exhibit a wet summer/dry winter cycle. Class 4 is characterized by moderate rainfall all year round, with a slight peak in late summer and fall. This includes much of the industrialized world: most of Europe, eastern North America, eastern Australia, and, arguably, Japan, as well as large parts of southern Asia and both major oceans. This seems to be a rather heterogeneous class, suggesting that more than six classes may be needed.

## 6. DISCUSSION

We have introduced the Bayesian morphology approach to image segmentation and the restoration of unordered-color images. For gray-level and multispectral images, this involves first segmenting the image using marginal mixture EM segmentation, and then applying discrete-valued ICM to the resulting segmentation. We have shown that discrete-valued ICM is equivalent to a form of mathematical morphology and that we can find the restoration corresponding to optimal parameter estimates without actually having to find these estimates. These two results provide considerable computational savings.

Bayesian morphology performs similarly to standard ICM in our experiments, but is much faster. In our gray-level image experiments, it was three to eight times faster, with the greater savings for the images requiring the most CPU time. In our experiments with multispectral images, the savings were even greater. For one 12-band image,

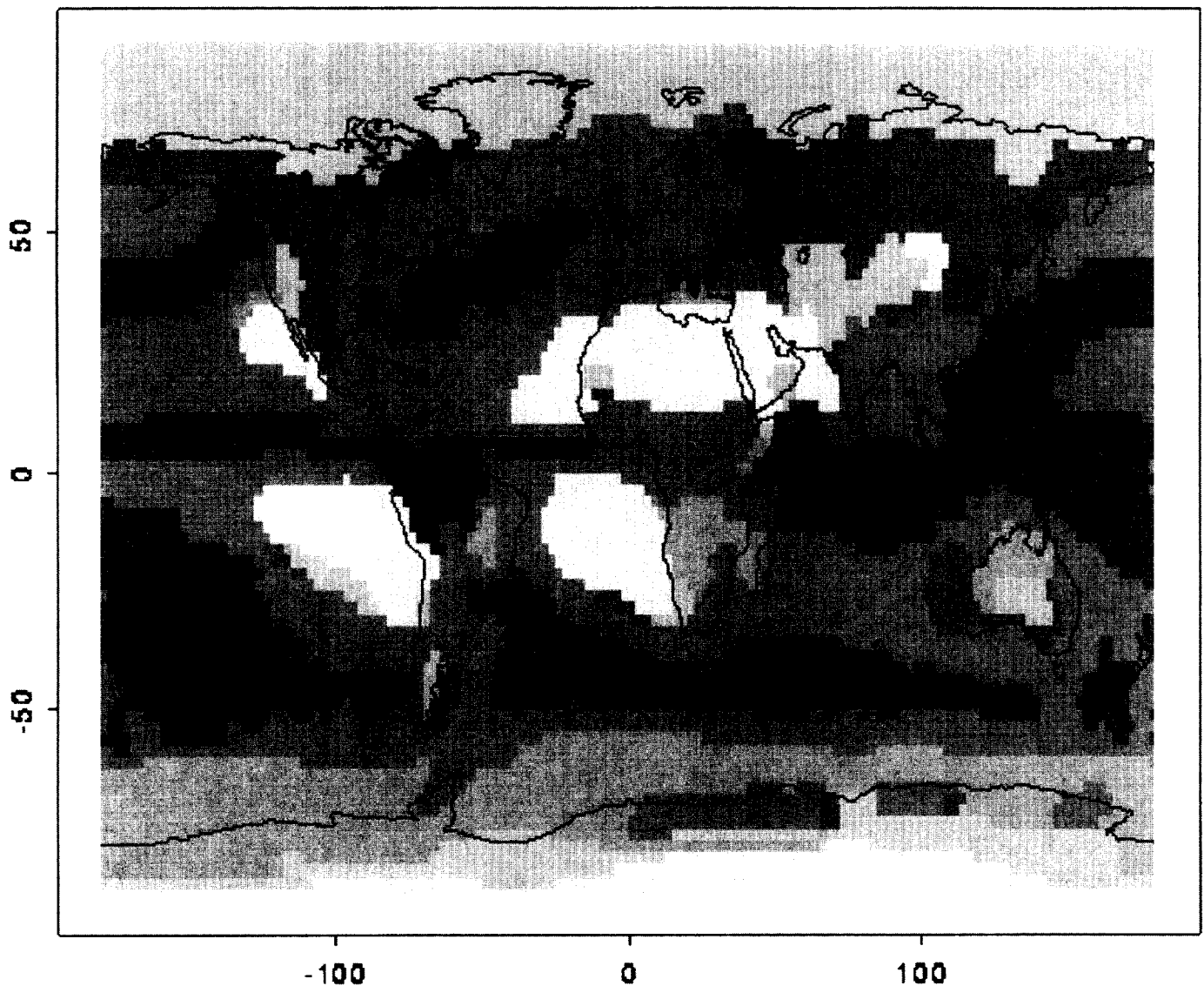


Figure 5. Bayesian Morphology Segmentation of the Legates/MSU Precipitation 12-Band Image, Modeling the Initial Marginal Mixture EM Segmentation as Being Degraded by Channel Noise. The initial value of  $\hat{w}$  was set to 1.

Bayesian morphology was more than 13 times faster than ICM. This opens the possibility of applying Bayesian image analysis in contexts where it has not been feasible before because of the great speed required, such as real-time and interactive image analysis and real-time video processing.

Bayesian morphology may also contribute improvements to the practice of mathematical morphology. This is already very fast and performs well; however, it lacks a formal statistical foundation for inference, and the specification of the sequence of morphological operations to be used is done in a rather ad hoc manner. Because Bayesian morphology is based on a statistical model, issues such as choice of a structuring element and choice of the sequence of morphological operations can be reduced to issues of statistical model selection and addressed, at least in principle, with Bayesian model selection by computing approximate Bayes factors (Ji and Seymour 1996; Kass and Raftery 1995).

A limitation of our study is that the insensitivity conditions we use seem to be limited to simple image and

noise models. It may be interesting to investigate further whether the analysis of more complex image models can be exactly or approximately divided into different steps involving unordered-color image restorations. Performing those restorations faster will then be relevant for a larger class of problems. For gray-level and multispectral images, one possible extension would be to iterate between the EM and ICM steps of the Bayesian morphology algorithm.

Another possible extension is the use of other models for the unobserved image. The Ising and Potts models do not always capture the image characteristics well enough. Other models have been proposed and studied by Descombes et al. (1995, 1996), and Tjelmeland and Besag (1998). These are higher-order interaction Markov random fields that involve three parameters regulating the presence of noise, edge, and line configurations. Each pixel is considered to have a  $5 \times 5$  neighborhood comprising the 24 nearest pixels. Such a neighborhood structure induces cliques that are  $3 \times 3$  squares. For binary Markov random fields, a configuration on a  $3 \times 3$  clique can be classified using the symmetries

(symmetry black–white, rotation) in one of 51 classes. A potential function is associated with each class, and constraints are imposed by relation between these functions. They involve three parameters,  $e$ ,  $l$ , and  $n$ . The parameters  $e$  and  $l$  can be interpreted as the edge and line energies per unit of length. The parameter  $n$  allows one to control the amount of noise. It is associated with noise configurations, typically those not involved in edge or line features. The resulting distribution has the form

$$\mathbb{P}(x) \propto \exp(-ev_0(x) - lv_1(x) - nv_2(x)),$$

where  $v_0$ ,  $v_1$ , and  $v_2$  depend on the  $3 \times 3$  configurations in  $x$ . In particular,  $v_2(x)$  is the number of noise configurations in  $x$ .

Our study can be easily extended to a one parameter version of these models. We can restrict ourselves to a situation where only the noise parameter  $n$  is unknown by setting the edge and line parameters to some constants. The reason for such a restriction is that insensitivity conditions still hold for models with several parameters, but it seems that there is no real gain from using them. Note that these models require more computation and, although they are more flexible, users may still prefer the limited but simple Potts model in most cases.

Other estimation criteria, such as those that take into account the observed image  $y$ , may also be worth investigating. Qian and Titterton (1992), estimated the parameters by maximizing

$$\prod_{i \in S} \mathbb{P}(y_i | \hat{x}_{S \setminus \{i\}}).$$

Focusing on  $\beta$  leads to equations similar to those in Section 4 (see Forbes and Raftery 1997), but the choice of an appropriate function  $f$  is not straightforward.

In addition, we believe that the morphological viewpoint can simplify the implementation of statistical algorithms such as ICM and give better insight into their convergence properties—in particular, through the properties of iterations of morphological transformations (see Heijmans 1994). This also includes considering alternatives to the commonly used Markov random fields priors, such as morphologically constrained Markov random fields (Sivakumar and Goutsias 1997). The latter incorporate geometric properties more clearly and may induce algorithms with clear morphological characteristics. Note that although our study and that of Sivakumar and Goutsias (1997) both attempt to link Bayesian image analysis and mathematical morphology, the goals and results are quite different. Sivakumar and Goutsias (1997) used ideas from mathematical morphology to try to build more complex and realistic Markov random field models for images. Applications of such models to texture simulation have been illustrated by Carstensen (1992). In our study, on the other hand, we have identified equivalences between simple and basic versions of both methodologies, and have tried to use them to find ways in which insights from each approach can yield improvements in the other one.

## REFERENCES

- Banfield, J. D., and Raftery, A. E. (1993), "Model-Based Gaussian and Non-Gaussian Clustering," *Biometrics*, 49, 803–821.
- Bensmail, H., and Celeux, G. (1996), "Regularized Gaussian Discriminant Analysis Through Eigenvalue Decomposition," *Journal of the American Statistical Association*, 91, 1743–1748.
- Besag, J. (1975), "Statistical Analysis of Non-Lattice Data," *The Statistician*, 24, 179–195.
- (1986), "On the Statistical Analysis of Dirty Pictures," *Journal of the Royal Statistical Society, Ser. B*, 48, 259–302.
- Besag, J., York, J., and Mollié, A. (1991), "Bayesian Image Restoration With Two Applications in Spatial Statistics," *Annals of the Institute of Statistical Mathematics*, 43, 1–59.
- Carstensen, J. M. (1992), "Description and Simulation of Visual Texture," Ph.D. thesis, Institute of Mathematical Statistics and Operations Research, Technical University of Denmark.
- Celeux, G., and Govaert, G. (1995), "Gaussian Parsimonious Clustering Models," *Pattern Recognition*, 28, 781–793.
- Comets, F., and Gidas, B. (1992), "Parameter Estimation for Gibbs Distributions From Partially Observed Data," *The Annals of Applied Probability*, 2(1), 142–170.
- Dasgupta, A., and Raftery, A. E. (1998), "Detecting Features in Spatial Point Processes With Clutter via Model-Based Clustering," *Journal of the American Statistical Association*, 93, 294–302.
- Descombes, X., Mangin, J.-F., Pechersky, E., and Sigelle, M. (1995), "Fine Structures Preserving Markov Model for Image Processing," *Proceedings of the 9th Scandinavian Conference on Image Analysis*, 349–356.
- Descombes, X., Morris, R., and Zerubia, J. (1996), "Estimation of Markov Random Field Prior Parameters Using Markov Chain Monte-Carlo Maximum Likelihood," Technical Report 3015, INRIA, Sophia Antipolis, France. Available at <http://www.inria.fr/rapports/sophia/RR-3015.html>.
- Forbes, F., and Raftery, A. E. (1997), "Bayesian Morphology: Fast Unsupervised Bayesian Image Analysis. Technical Report 325, University of Washington, Dept. of Statistics. Available at <http://www.stat.washington.edu/tech.reports/tr325.ps>.
- Fovell, R. G. (1997), "Consensus Clustering of U.S. Temperature and Precipitation Data," *Journal of Climate*, 10, 1405–1427.
- Geman, S., and Geman, D. (1984), "Stochastic Relaxation, Gibbs Distributions and the Bayesian Restoration of Images," *IEEE Transactions on Pattern Analysis and Machine Intelligence*, 6, 721–741.
- Georgii, H. O. (1988), *Gibbs Measures and Phase Transitions*, Berlin: de Gruyter.
- Geyer, C. J. (1991), "Reweight Monte Carlo Mixtures," Technical Report 568, University of Minnesota, School of Statistics.
- Geyer, C. J., and Thompson, E. A. (1992), "Constrained Monte Carlo Maximum Likelihood for Dependent Data" (with discussion), *Journal of the Royal Statistical Society, Ser. B*, 54, 657–699.
- Gidas, B. (1993), "Parameter Estimation for Gibbs Distributions From Fully Observed Data," in *Markov Random Fields—Theory and Applications*, eds. R. Chellapa and A. Jain, Boston: Academic Press, pp. 471–498.
- Goutsias, J. K. (1991), "Unilateral Approximation of Gibbs Random Field Images," *Computer Vision, Graphics and Image Processing: Graphical Models and Image Processing*, 53, 240–257.
- Heijmans, H. J. (1994), *Morphological Image Operators*, Boston: Academic Press.
- Hummel, R. A., and Zucker, S. W. (1983), "On the Foundations of Relaxation Labelling Processes," *IEEE Transactions on Pattern Analysis and Machine Intelligence*, 5, 267–287.
- Ji, C., and Seymour, L. (1996), "A Consistent Model Selection Procedure for Markov Random Fields Based on Penalized Pseudolikelihood," *Annals of Applied Probability*, 6, 423–443.
- Kass, R. E., and Raftery, A. E. (1995), "Bayes Factors," *Journal of the American Statistical Association*, 90, 773–795.
- Matheron, G. (1975), *Random Sets and Integral Geometry*, New York: Wiley.
- Posse, C. (1998), "Hierarchical Model-Based Clustering for Large Data Sets," unpublished manuscript, University of Minnesota, Dept. of Statistics.
- Qian, W., and Titterton, M. (1992), "Stochastic Relaxations and EM Algorithms for Markov Random Fields," *Journal of Statistical Computation and Simulation*, 40, 55–69.

[Received December 1997. Revised September 1998.]

- Rosenfeld, A., Hummel, R. A., and Zucker, S. W. (1976), "Scene Labelling by Relaxation Operation," *IEEE Transactions on Systems, Man and Cybernetics*, 6, 420-433.
- Serra, J. (1982), *Image Analysis and Mathematical Morphology*, New York: Academic Press.
- Sivakumar, K., and Goutsias, J. K. (1997), "Morphologically Constrained Discrete Random Sets," in *Advances in Theory and Applications of Random Sets*, ed. D. Jeulin, Singapore: World Scientific Publishing Company.
- Swendsen, R. H., and Wang, J. S. (1987). "Nonuniversal Critical Dynamics in Monte Carlo Simulations," *Physical Review Letters*, 58, 86-88.
- Tjelmeland, H. (1996), "Stochastic models in reservoir characterization and Markov random fields for compact objects," Ph.D. thesis, Norwegian University of Science and Technology, Dept. of Mathematical Sciences.
- Tjelmeland, H., and Besag, J. (1998), "Markov Random Fields With Higher Order Interactions," *Scandinavian Journal of Statistics*, 25, 415-434.
- Zhang, B., Shirazi, M. N., and Noda, H. (1996), "Blind Restoration of Degraded Binary Markov Random Field Images," *Graphical Models and Image Processing*, 58, 90-98.